Hindawi Publishing Corporation
Advances in Materials Science and Engineering
Volume 2016, Article ID 6375131, 10 pages
http://dx.doi.org/10.1155/2016/6375131

Research Article

Experimental and Numerical Investigations of Fretting Fatigue Behavior for Steel Q235 Single-Lap Bolted Joints

Yazhou Xu, Zhen Sun, and Yuqing Zhang

School of Civil Engineering, Xi'an University of Architecture and Technology, Shaanxi 710055, China

Correspondence should be addressed to Yazhou Xu; yazhou_xhu@163.com

Received 6 June 2016; Revised 17 August 2016; Accepted 21 August 2016

Academic Editor: Antônio G. de Lima

This work aims to investigate the fretting fatigue life and failure mode of steel Q235B plates in single-lap bolted joints. Ten specimens were prepared and tested to fit the *S-N* curve. SEM (scanning electron microscope) was then employed to observe fatigue crack surfaces and identify crack initiation, crack propagation, and transient fracture zones. Moreover, a FEM model was established to simulate the stress and displacement fields. The normal contact stress, tangential contact stress, and relative slipping displacement at the critical fretting zone were used to calculate FFD values and assess fretting fatigue crack initiation sites, which were in good agreement with SEM observations. Experimental results confirmed the fretting fatigue failure mode for these specimens. It was found that the crack initiation resulted from wear regions at the contact surfaces between plates, and fretting fatigue cracks occurred at a certain distance away from hole edges. The proposed FFD-*N* relationship is an alternative approach to evaluate fretting fatigue life of steel plates in bolted joints.

1. Introduction

Bolted joints are widely used in many engineering structures directly subjected to dynamic loads, while fatigue failure is a major failure mechanism for these joints. In particular, there are a few contact surfaces in bolted connections, in which microslip at the interfaces inevitably occurs under cyclic loading. The wear damage and fretting damage due to the microslip between the contact surfaces thus lead to fretting fatigue failure. Although many works related to fretting fatigue life have been conducted experimentally and numerically, it is still an open problem due to its intrinsical complexity. In fact, fretting fatigue is heavily sensitive to material properties, joined details, wear, corrosion, and so forth. It still meets tremendous difficulties to assess fretting fatigue life quantitatively.

Chakherlou et al. investigated the effect of clamping force on the fatigue life of bolted plates by means of testing and 3D finite element method. They found that the compressive stresses around plate holes were beneficial to the fatigue life of bolted plates, and the improvement was more effective in the high cycle life region [1]. However, the increase of clamping force would induce fretting damage due to high contact stresses. Lee et al. conducted a test to investigate the fretting fatigue behavior of cavitation shotless peened titanium alloy (Ti–6Al–4V), and numerical analysis based on finite element code ABAQUS was performed [2]. Moreover, aluminum alloy specimens made of 7075-T6 with bolted cold expanded hole were tested. The fatigue life and the effect of clamping force on the residual stress distribution resulting from cold expansion were investigated [3]. The results indicated that the failure mode changed from notch fatigue to fretting fatigue. Also, Chakherlou et al. studied the lubricating effect on friction of aluminum alloy shear lap joints with different clamping forces [4]. Furthermore, the fatigue lives of interference fitted-bolt clamped double-lap joints and bolted/bonded connected hybrid joints [5] were evaluated via test and numerical analysis. Recently, Rahmat et al. studied the fretting life of Al7075-T6 considering the combined effect of fretting and notch. The fractographic analysis demonstrated that the crack initiation resulted from fretting damage [6].

Some researchers also dealt with fretting fatigue of single-lap joints. Starikov investigated the fatigue life of single overlap fastened aluminum joints under FALSTAFF spectrum

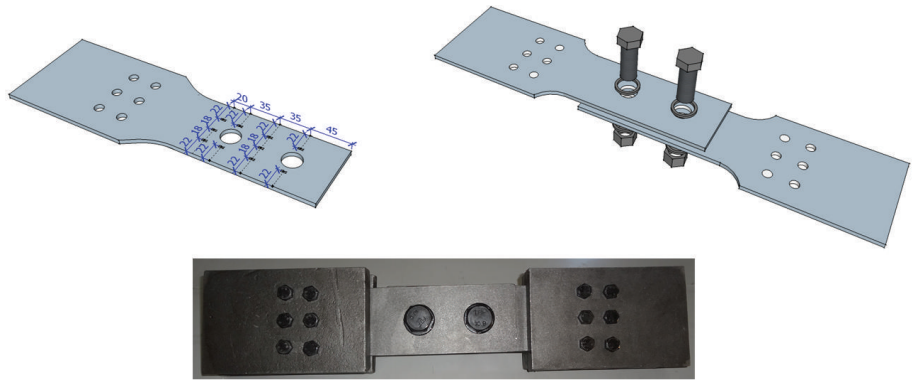

Figure 1: Schematic of specimens and the assembling, dimensions in mm.

blocks [7]. Hoang and his coworkers investigated the failure mode of a bolted single-lap joint under tension-shearing [8]. Ju et al. also studied a butt-type bolted steel connection using finite element method; they found that linear fracture mechanics was still adaptive to the bolted joint problem in spite of its highly nonlinear structural behavior [9].

In addition, the fretting fatigue behavior of a steel-aluminum bolted assembly was studied by testing and finite element analysis. The fretting mechanism at the interface connected different materials was analyzed by means of scanning electron microscope (SEM) and energy dispersive spectrometer (EDS) [10]. Maximov et al. developed a fabrication process by which beneficial residual hoop compressive stresses around the bolt hole were almost uniformly distributed along the axis of the holes, so that the fatigue life of the net section in fitted-bolt connections was increased [11]. Liu et al. used two critical plane models to predict the fatigue life of bolted aluminum alloy joints subjected to different stress ranges, and the results were compared to the experimental values [12]. Hobbs et al. investigated the effect of eccentricity on the fatigue life of bolts. Their results indicated that the eccentric load reduced the fatigue life of bolts, which was proportional to the enhancement of the local stress amplitude induced by the eccentricity [13]. Using a 2D finite element model, Hojjati-Talemi et al. employed continuum damage mechanics to predict the crack initiation of specimens made of aluminum alloy 7075-T6 in contact with square-angled pads; extended finite element (XFEM) analysis was then carried out to predict crack propagation life [14].

Oskouei and Ibrahim improved the fretting fatigue performance of Al 7075-T6 bolted plates by using electroless Ni-P coatings with a thickness of 40 μm [15]. They reported that there was good adhesion between the Al substrate and Ni-P deposit at low and moderate loads, while fracture and delaminations of the coating film at high cyclic loads occurred. Furthermore, the effects of clamping pressure and friction force on the fretting fatigue performance of Al 7075-T6 bolted plates with electroless Ni-P coatings were examined based on a 2D finite element model, in which Ni-P coatings with thickness of 40 μm were separately modeled with fine meshes, and the mechanical properties were determined using nanoindentation method [16]. Recently, Oskouei et al. also investigated the surface roughness and chemical phase composition of the fretting damaged zone for Al 7075-T6 bolted plates; the influence of fretting fatigue damage on the surface roughness for Ni-P coated and uncoated Al 7075-T6 bolted plates was examined [17].

As mentioned above, most of the existing works focused on the fretting life of Al or Ti alloy bolted plates commonly used in mechanical and aerospace industries. This work aims to investigate the failure mechanism of steel bolted single-lap steel joints, which is often used in civil engineering. This paper is organized as follows. The specimen preparation and testing plan are described in Section 2. Next, the fatigue testing results and SEM analysis are presented in Section 3. In Section 4, numerical simulations using finite element method are conducted. Finally, some conclusions are drawn in Section 5.

2. Specimens Preparation and Testing Procedure

2.1. Testing Specimens. Ten specimens made of commercial steel Q235B, with chemical composition expressed in percentage (wt.%) as Si 0.03, Mn 0.28, P 0.012, C 0.18, and S less than 0.005 provided by the manufacturer, were manufactured to conduct fretting fatigue tests. Additionally, two specimens were used to test mechanical properties such as yielding strength, Young's modulus, and ultimate strength. The distance between bolts and edge position satisfied the specification in [18]. The specimens were designed as "dog bone" configuration with two bolts. The detailed sizes and assembly are shown in Figure 1. The specimen had two drilled holes with a diameter of 22 mm. The contact surfaces were treated by the sand-blast method to improve the friction at the interface. Two M20 hexagon-head bolts of strength class 10.9 fastened the plates both with thickness of 5 mm. By using a wrench, the expected clamping force was achieved with torque of 435 N·m, corresponding to pretension force of 155 kN and torque coefficient of 0.14. We employed the same wrench and operational procedure to ensure approximately equal torque or clamping force for each specimen.

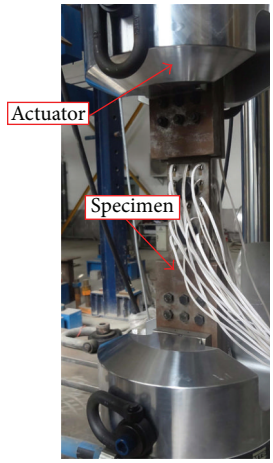

Figure 2: Experimental setup of the fretting fatigue test.

2.2. Testing Setup. In this work, tensile test, fatigue test, and microscopic test (scanning electron microscope) were utilized to obtain material parameters and fatigue life and identify the microscopic mechanism of the fretting fatigue failure, respectively.

Firstly, the tensile test for steel Q235B aimed to obtain mechanical properties, such as Young's modulus, yielding strength, and ultimate strength. These parameters were used to evaluate the stress ranges in the following fatigue test, also implemented in the finite element model in Section 4. In addition, the tensile test for an assembled specimen was also conducted to assess the critical slipping load, which corresponded to the frictional slipping failure at the macro level.

Fretting fatigue testing of ten specimens was then carried out by using MTS-50 hydroserve machine. Figure 2 displayed the testing instrument. The cyclic loading was constant amplitude harmonic waves at a frequency of 30 Hz, and the stress ratio $R = 0.1$. To avoid slipping failure modes between two plates, the maximum loads were controlled at less than 95 kN, obtained from the previous tensile test of the assembled specimen.

Fractographic analyses were consequently carried out on four typical fractured specimens utilizing a scanning electron microscope (JEOL JSM-6460). The SEM specimens were prepared by means of line cutting, alcohol rinsing, and air-drying. We particularly focused on the fatigue crack initiation sites, fretting wear damage, and characteristics of facture zones.

3. Experimental Results and Discussions

3.1. Tensile Test. The specimens for the tensile test were made of commercial steel plate designated as Q235B in accordance with [19]. The detailed experimental results are listed in Table 1.

3.2. Fretting Fatigue Testing Results. As mentioned previously, the maximum loading amplitude was restrained according to the tensile testing for an assembled specimen to realize the expected fretting fatigue failure mode, rather than the slipping failure at the contact surfaces. All ten specimens exhibited wear damage in the contact regions between washers and plates. Among them, eight specimens fractured due to fretting fatigue cracks. The test for the other two specimens was terminated when the loading cycles reached 1*E*7. Herein, the specimen with the stress range of 125 MPa did not fracture, which was designed to determine the fatigue durance. Next, the stress range was increased up to 137.5 MPa; the failure of the specimen was due to fatigue cracks. Then, the stress range was decreased to 131.25 MPa; fatigue failure did not occur when the life reached 1*E*7. Since the relative deviation between 137.5 MPa and 131.25 MPa was less than 5% and the main objective of this work was not to determine the fatigue durance life accurately, the fatigue durance of the connection was then evaluated as the average of 137.5 MPa and 131.25 MPa, that is, 134.4 MPa. The tested fatigue lives subjected to different stress ranges are shown in Figure 3. Correspondingly, the *S*-*N* relationship was fitted in terms of experimental results (see (1)). The final cracks of seven specimens and wear damage are shown in Figure 4, in which specimen S9 corresponds to fatigue life of 1*E*7.

Table 1: Experimental mechanical properties of steel Q235B.

Yielding strength (MPa)	Ultimate strength (MPa)	Young's modulus (MPa)
317.7	476.6	1.96*E*5

$$S = 132.2\left(1 + \frac{12156.26}{N^{0.8384}}\right). \quad (1)$$

It was observed that all fatigue cracks propagated across the wear regions between the plates. The final crack sites were away from the hole edges, which were close to the actuator. The characteristic of the fractography morphology demonstrates that the fatigue cracks originate from the fretting effect at the contact surfaces and propagate toward the side edges parallel to the loading direction. It was also observed that iron oxide powders dropped down at the fixed bottom end during cyclic loading. There were marron red wear zones around the fatigue crack sources for all specimens. Particularly, the fretting damage was more severe as the fatigue life was longer, corresponding to smaller stress ranges.

3.3. Fractographic Observations. Since the fracture zone was approximately symmetric about the central axis, half a fracture surface of each specimen was scanned in the following tests, and each scanned fracture surface consisted of four subregions. The SEM images for a fracture surface with different magnification times are shown in Figure 5.

It was found that the fretting fatigue initiation exhibited a multisource characteristic, and the fatigue crack initiation sites occurred at the middle contact surfaces between the plates. Then, the crack propagated toward the two side edges and the opposite surface. As the crack length reached a critical size, the specimen fractured rapidly. In most cases, the specimens did not fracture completely since the loading machine

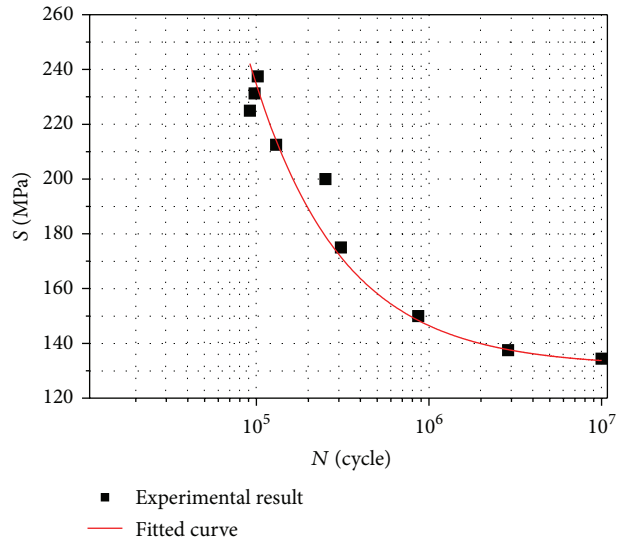

Figure 3: Experimental fatigue lives and fitted *S*-*N* relationship.

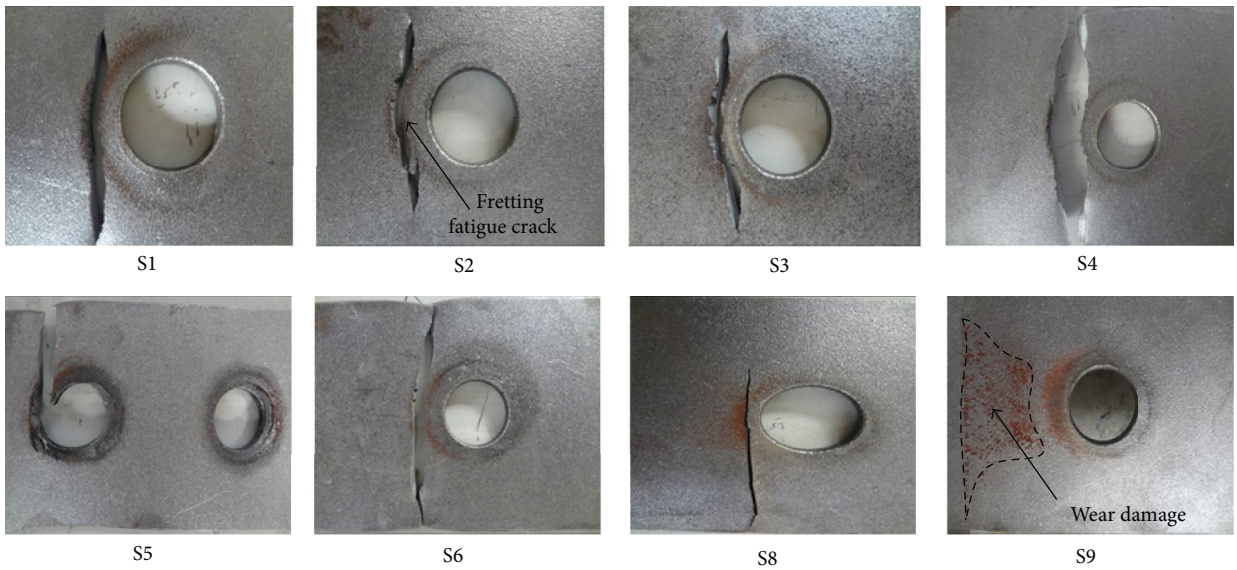

Figure 4: Illustration of fatigue fracture surfaces and fretting damage at the contact surfaces.

was programmed not to run beyond 1 mm for its protection. The fatigue crack initiation zone, propagation zone, and transient fracture zone for a specimen are illustrated in Figure 5. The fatigue crack initiation zone is smooth and bright in comparison to other sites. It is worth noting that the fracture surfaces become smoother with the increase of the fatigue life.

4. Finite Element Analysis

4.1. Finite Element Model. Since the fretting fatigue crack of bolted joints often initiates at the contact surfaces between plates, it is difficult to observe the crack initiation, propagation, and fracture process and measure strain and relative slipping at the critical interface directly. Besides, the fatigue test is often time-consuming and expensive. Thus, finite element method is often used to interpret experimental results and conduct parameter analysis. Keikhosravy et al. utilized a 3D finite element model validated by the monotonously tensile testing results to investigate the effect of geometric sizes on the stress distribution in Al 2024-T3 single-lap joints with one bolt. And it was found that the parameters of plates' width and edge distance influenced the stress distribution in accordance with different failure modes [20]. Additionally, the Mises stress distribution on the hole circumference and shifting of failure modes of Al 2024-T3 in double-lap bolted joints with single and double fasteners were also

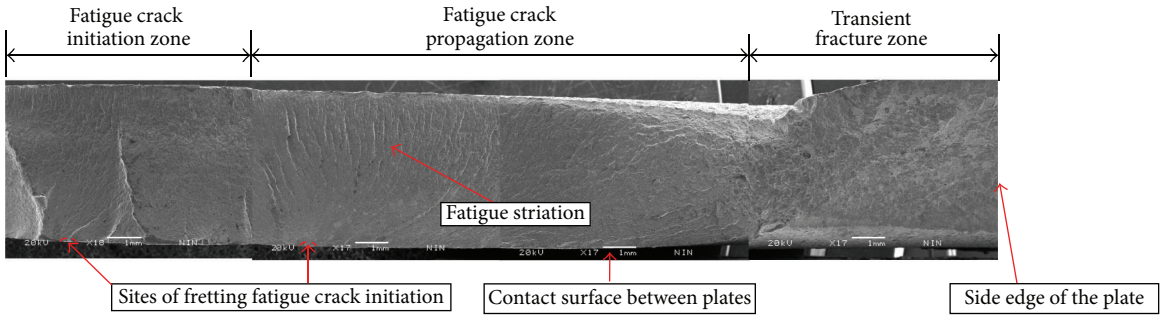

(a)

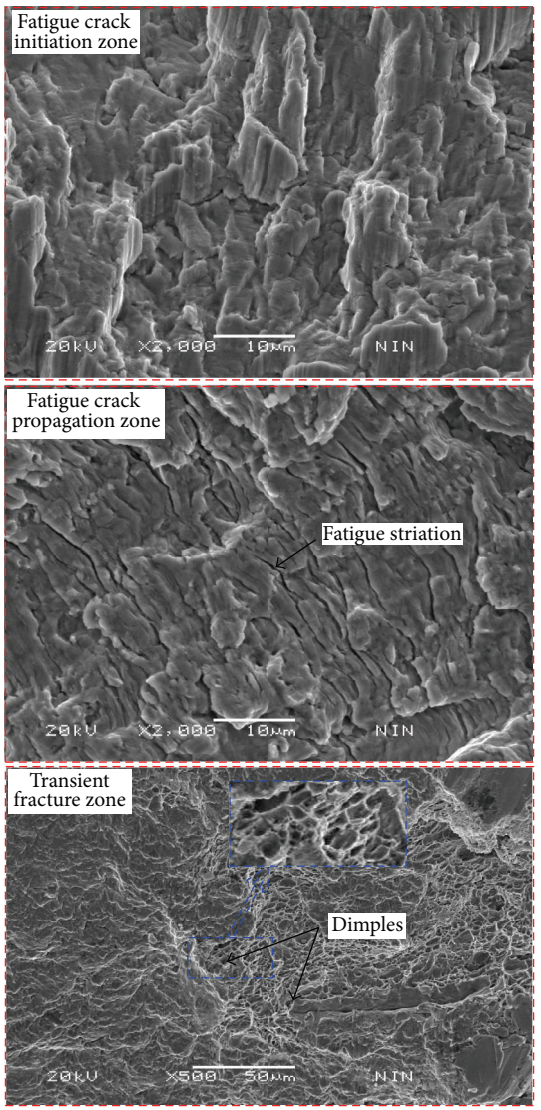

(b)

Figure 5: SEM images of a fracture surface (fatigue life = 865471; the left is near the middle of the plate, and the right is close to the side edge); (a) fractured surface (lower magnification); (b) fractured surfaces at crack initiation, crack propagation, and transient fracture zones (higher magnification).

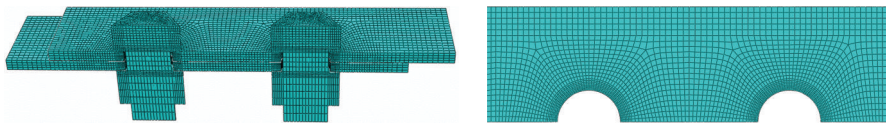

(a) Mesh of half assembled model (b) Refined mesh around plate holes

Figure 6: Mesh of the FEM model and refined mesh around holes.

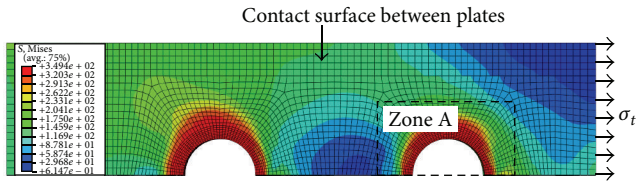

Figure 7: Mises stress distribution on the contact surface between plates (σ_t = 175 MPa).

investigated [21]. Nevertheless, the bearing failure mode of specimens in this work has been prevented by limitation of the maximum tensile load; more experimental and numerical works need to be conducted, in order to further clarify the effect of geometric parameters, clamping force, and friction coefficient on the failure modes of this type of joint.

In this section, a finite element model was developed by ABAQUS software package to predict the stress and relative slipping in the critical region. Based on the calculated normal contact stress, tangential contact stress, and relative slipping displacement, the fretting fatigue life could be reasonably assessed. Similarly, taking advantage of the symmetry, only 1/2 geometry was modeled in this paper. And it was easily understood that the bolted joints would be the failure region, so that the ends of the assembled specimens were excluded from the finite element models in order to improve the simulation convergence and efficiency. Herein, a gap of 1 mm existed between the bolt shanks and holes in the plates. And the mesh around the holes was refined to deal with the stress concentration. Typical meshes are shown in Figure 6.

The simulation considering contact problems is sensitive to the boundary conditions and loading rules. In the present model, one end of the FE model along the loading direction was fixed, and the other end was loaded with uniform tensile stress. Due to the symmetry, sliding boundary conditions along the loading direction were imposed to the symmetry surfaces, which meant that the plates could deform along the loading direction and keep fixed in the other two directions. There were four contact pairs in the models, in order to simulate the contact interactions including washer/plate (hard contact), plate/plate (with contact coefficient of 0.45), plate/washer (hard contact), and washer/nut (hard contact). Additionally, the clamping forces were simulated by means of the bolt load provided in ABAQUS. In the first step, a small clamping force (10 N) was loaded. In the next step, the clamping force was increased up to the specified values. Then, the uniform tensile stress was exerted at the end of the plate, while the bolt load was assigned to keep the same length at the previous step.

The constitutive law for bolts and washers was linear and isotropic, while the plates were modeled with an elastoplasticity stress-strain relationship measured from the previous tensile test. The elements were modeled with C3D8R.

4.2. FEM Simulation Results. To simulate and interpret the experimental results, stress and relative sliding distributions in the contact zones between plates were mainly investigated, as the fretting fatigue crack initiation occurred in the contact interfaces according to the SEM observation. Figure 7 shows the Mises stress distribution on the contact surface between plates with a stress range of 175 MPa. One can find that the stress concentration occurs around the holes, and the maximum Mises stress is two times larger than the far field uniform stress. From the experimental results, we have found that nearly all specimens fractured in the contact zones between the plates adjacent to the loading end (see Figure 7); the local zone around the hole (dashed line enclosed in Figure 7) is hence analyzed in detail. The normal contact stress, tangential contact stress, and relative slipping displacement perpendicular to the fracture surface are shown in Figures 8(b), 8(c), and 8(d), respectively. Consequently, the stress distribution and relative slipping in the potential crack initiation sites numbered 1 to 13 (see Figure 8(a)) are further investigated. The normal contact stress, tangential contact stress, and relative slipping displacement of the nodes subjected to different stress ranges are shown in Figures 8(b), 8(c), and 8(d), respectively. It is easy to see that there is heavy stress concentration around the holes due to the clamping force.

By calculating FFD values at the contact surface, we found that the nodes labelled from 1 to 13 at Zone A (see Figure 8(a)) were the most possible crack initiation sites, in accordance with the SEM results. Hence, the distributions of the stress and relative slipping displacement at these nodes were investigated in detail and shown in Figures 9(a), 9(b), and 9(c), respectively.

As seen in Figure 9, the normal contact stresses decrease from Node 1 to Node 13 as a whole, but there are still local peaks. Furthermore, the maximum tangential contact stresses

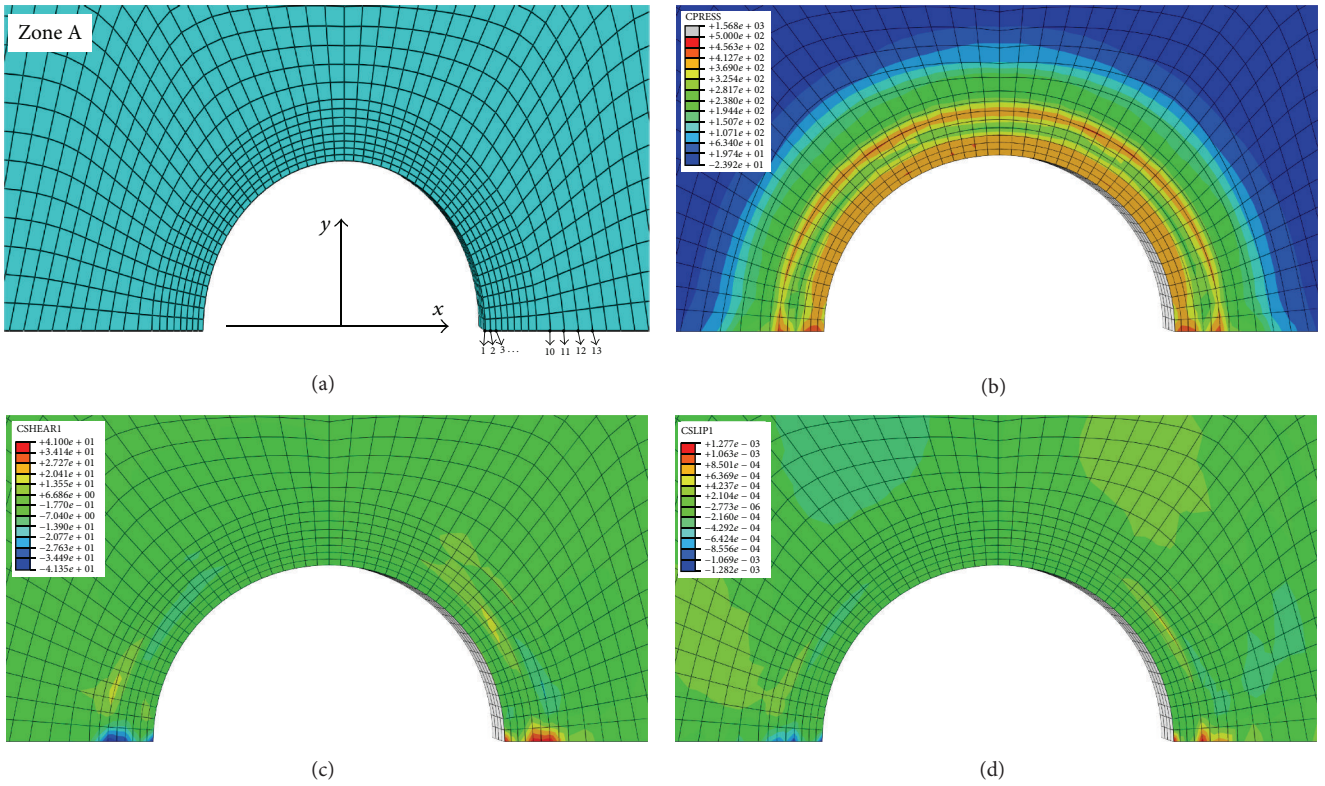

FIGURE 8: Contact stress and slipping distribution on the contact surface between plates (σ_t = 175 MPa). (a) Node label; (b) normal contact compression stress; (c) tangential contact stress along to the loading direction (x-axis); (d) relative slipping displacement.

uniformly occur at Node 10. In contrast, the relative slipping displacement roughly increases from Node 1 to Node 13. As well known, the fretting fatigue crack heavily depends on the relative slipping and friction force. So, we predict the fretting fatigue crack initiation in terms of the FFD parameter in the next section.

4.3. Fretting Fatigue Predicated by FFD. FFD [22] parameter is defined as

$$\mathrm{FFD} = \mu \times |\sigma_n| \times |\delta| \times \sigma_r, \tag{2}$$

where μ denotes the friction coefficient, σ_n is the normal contact stress, σ_r is the tangential contact stress, and δ stands for the relative slipping displacement. Herein, we calculate the FFD values for the nodes based on the FEM results in Section 4.2. The FFD values of different nodes subjected to different stress ranges are shown in Figure 10. It is found that the FFD coincidently reaches its maximum in Node 10, which matches the experimental fracture sites well for most specimens, approximately 5 mm away from the hole edges. Moreover, one can predict the fretting fatigue life based on the FFD parameter. For different loading cases, the maximum FFD-fretting fatigue life curve is plotted in Figure 11. Correspondingly, the maximum FFD-fretting fatigue life relationship is formulated by (3); FFD exhibits good relevancy with fretting fatigue life.

$$\mathrm{FFD}_{\max} = 11.87\left(1 + \frac{10^{9.97044}}{N^{1.80287}}\right). \tag{3}$$

5. Conclusions

Ten bolted single-lap joints made of Q235 steel were prepared to investigate the fatigue behavior. It is found that all specimens exhibit wear and fretting damage. The experimental phenomena show that fretting damage exists at the contact surfaces between the plates, where the crack initiation consequently forms with the damage accumulation due to the fretting wear. And the SEM observation of the crack surfaces also demonstrated that the crack nucleation indeed locates at the contact surfaces between plates. Then, the microcrack spreads toward the two sides and the opposite surface. Finally, the specimens rupture as the residual section could not withstand the tensional stress. In addition, the fatigue life endurance is also evaluated.

Based on the experimental fatigue life, an analytical formula is established to fit the S-N relationship. By means of FEM simulation, normal contact stress, tangential contact stress, and relative slipping displacement are investigated, and in particular their distributions at the critical contact zone are discussed in detail. Based on the numerical results, the

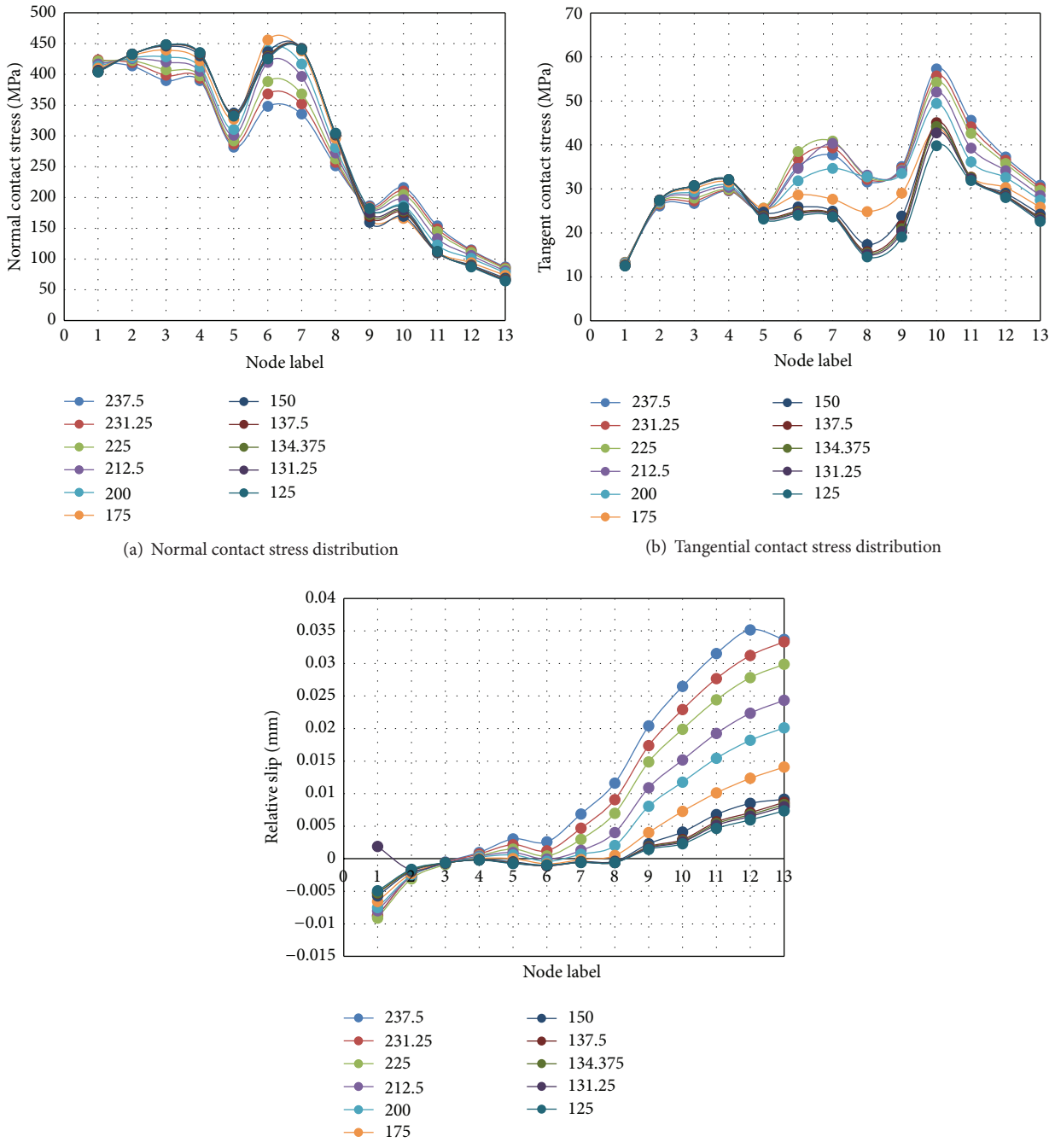

(a) Normal contact stress distribution

(b) Tangential contact stress distribution

(c) Relative slipping distribution of the contact surface between plates

FIGURE 9: Distribution of normal stress and tangential contact stress and slipping at different nodes.

fretting fatigue crack initiation at contact interfaces is successively predicted by using corresponding FFD values, and the proposed FFD-N formula could be an alternative way to evaluate the fretting fatigue life of bolted single-lap connections.

Competing Interests

The authors declare that there are no competing interests regarding the publication of this paper.

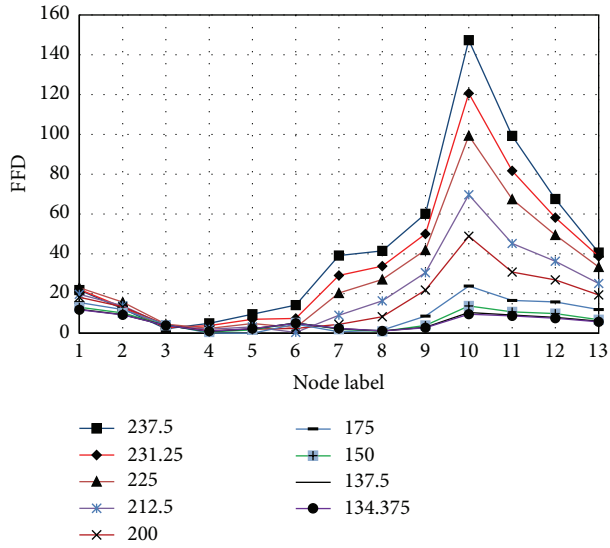

Figure 10: FFD distribution subjected to different stress ranges.

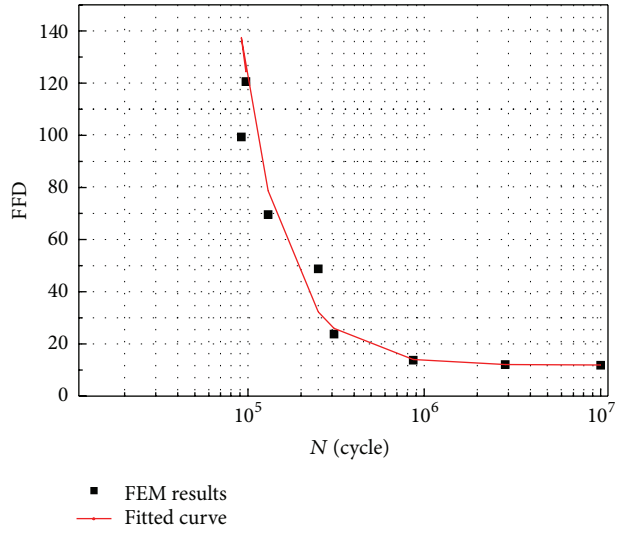

Figure 11: FFD-N relationship.

Acknowledgments

The support of the Natural Science Foundation of China (Grants nos. 51208410 and 51578444) and the Ministry of Education Plan for Yangtze River Scholar and Innovation Team Development (no. IRT13089) is gratefully acknowledged. Innovation Team Plan of Xi'an University of Architecture and Technology is also acknowledged.

References

[1] T. N. Chakherlou, R. H. Oskouei, and J. Vogwell, "Experimental and numerical investigation of the effect of clamping force on the fatigue behaviour of bolted plates," *Engineering Failure Analysis*, vol. 15, no. 5, pp. 563–574, 2008.

[2] H. Lee, S. Mall, and H. Soyama, "Fretting fatigue behavior of cavitation shotless peened Ti–6Al–4V," *Tribology Letters*, vol. 36, no. 2, pp. 89–94, 2009.

[3] T. N. Chakherlou, Y. Alvandi-Tabrizi, and A. Kiani, "On the fatigue behavior of cold expanded fastener holes subjected to bolt tightening," *International Journal of Fatigue*, vol. 33, no. 6, pp. 800–810, 2011.

[4] T. N. Chakherlou, M. J. Razavi, A. B. Aghdam, and B. Abazadeh, "An experimental investigation of the bolt clamping force and friction effect on the fatigue behavior of aluminum alloy 2024-T3 double shear lap joint," *Materials & Design*, vol. 32, no. 8-9, pp. 4641–4649, 2011.

[5] F. Esmaeili, T. N. Chakherlou, and M. Zehsaz, "Investigation of bolt clamping force on the fatigue life of double lap simple bolted and hybrid (bolted/bonded) joints via experimental and numerical analysis," *Engineering Failure Analysis*, vol. 45, pp. 406–420, 2014.

[6] M. A. Rahmat, R. N. Ibrahim, and R. H. Oskouei, "A study on the combined effect of notch and fretting on the fatigue life behaviour of Al 7075-T6," *Materials & Design*, vol. 60, no. 8, pp. 136–145, 2014.

[7] R. Starikov, "Fatigue behaviour of mechanically fastened aluminium joints tested in spectrum loading," *International Journal of Fatigue*, vol. 26, no. 10, pp. 1115–1127, 2004.

[8] T. D. Hoang, C. Herbelot, and A. Imad, "On failure mode analysis in a bolted single lap joint under tension-shearing," *Engineering Failure Analysis*, vol. 24, no. 5, pp. 9–25, 2012.

[9] S.-H. Ju, C.-Y. Fan, and G. H. Wu, "Three-dimensional finite elements of steel bolted connections," *Engineering Structures*, vol. 26, no. 3, pp. 403–413, 2004.

[10] A. Benhamena, A. Talha, N. Benseddiq, A. Amrouche, G. Mesmacque, and M. Benguediab, "Effect of clamping force on fretting fatigue behaviour of bolted assemblies: case of couple steel–aluminium," *Materials Science and Engineering A*, vol. 527, no. 23, pp. 6413–6421, 2010.

[11] J. T. Maximov, G. V. Duncheva, and N. Ganev, "Enhancement of fatigue life of net section in fitted bolt connections," *Journal of Constructional Steel Research*, vol. 74, no. 6, pp. 37–48, 2012.

[12] J. Liu, J. X. Kang, W. Z. Yan, F. S. Wang, and Z. F. Yue, "Prediction of fatigue performance of fastener holes with bolt clamping force based on critical plane approach," *Materials Science and Engineering A*, vol. 527, no. 15, pp. 3510–3514, 2010.

[13] J. W. Hobbs, R. L. Burguete, P. F. Heyes, and E. A. Patterson, "The effect of eccentric loading on the fatigue performance of high-tensile bolts," *International Journal of Fatigue*, vol. 22, no. 6, pp. 531–538, 2000.

[14] R. Hojjati-Talemi, M. A. Wahab, E. Giner, and M. Sabsabi, "Numerical estimation of fretting fatigue lifetime using damage and fracture mechanics," *Tribology Letters*, vol. 52, no. 1, pp. 11–25, 2013.

[15] R. H. Oskouei and R. N. Ibrahim, "Improving fretting fatigue behaviour of Al 7075-T6 bolted plates using electroless Ni-P coatings," *International Journal of Fatigue*, vol. 44, pp. 157–167, 2012.

[16] M. A. Rahmat, R. N. Ibrahim, and R. H. Oskouei, "A stress-based approach to analyse fretting fatigue life behaviour of electroless Ni–P coated Al 7075-T6," *Materials Science and Engineering A*, vol. 631, pp. 126–138, 2015.

[17] R. H. Oskouei, M. R. Barati, and R. N. Ibrahim, "Surface characterizations of fretting fatigue damage in aluminum alloy 7075-T6 clamped joints: the beneficial role of Ni–P coatings," *Materials*, vol. 9, no. 3, article 141, 2016.

[18] JGJ82-91, Design, construction and acceptance specification for high strength bolt connection of steel structure, 1991.

[19] GB-50017, "Code for design for steel structure," 2003.

[20] M. Keikhosravy, R. H. Oskouei, P. Soltani, A. Atas, and C. Soutis, "Effect of geometric parameters on the stress distribution in Al 2024-T3 single-lap bolted joints," *International Journal of Structural Integrity*, vol. 3, no. 1, pp. 79–93, 2012.

[21] K. Fallahnezhad, A. Steele, and R. H. Oskouei, "Failure mode analysis of aluminium alloy 2024-T3 in double-lap bolted joints with single and double fasteners; a numerical and experimental study," *Materials*, vol. 8, no. 6, pp. 3195–3209, 2015.

[22] C. Ruiz, P. H. B. Boddington, and K. C. Chen, "An investigation of fatigue and fretting in a dovetail joint," *Experimental Mechanics*, vol. 24, no. 3, pp. 208–217, 1984.